Air Pollution Modelling Using Finite Diference in a Terrain Conformal Coordinate System

G. Montero [a], N. Sanín [a]

[a] *University Institute of Intelligent Systems and Numerical Applications in Engineering (IUSIANI), University of Las Palmas de Gran Canaria, Spain.*
gustavo@dma.ulpgc.es

Abstract

A 3-D model for pollutant transport is proposed considering a set of coupled convection-diffusion-reaction equations. The convective phenomenon is mainly produced by a wind field obtained from a 3-D mass consistent model. In particular, the modelling of oxidation and hydrolysis of sulphur and nitrogen oxides released to the surface layer is carried out by using a linear module of chemical reactions. Dry deposition process is represented by the so-called deposition velocity, introduced as a boundary condition. Wet deposition is included in the source term of the governing equations using the washout coefficient.

To obtain a numerical solution the problem is transformed before using a conformal coordinates system. This allows to work with a simpler domain in order to build a mesh that provides high consistency finite difference schemes. The convection-diffusion-reaction equations are solved using a high order time discretization which is obtained following the technique of Lax and Wendroff. Finally, the model is tested with a numerical experiment in La Palma Island (Canary Islands).

Key words: Wind modelling, mass consistent models, air pollution model, eulerian model, finite differences, accurate time-stepping.

1 Wind field approach

The continuity equation and the impermeability conditions on the terrain Γ_b are, respectively

$$\vec{\nabla} \cdot \vec{u} = 0 \ \text{ in } \ \Omega \tag{1}$$

$$\vec{n} \cdot \vec{u} = 0 \ \text{ in } \ \Gamma_b \tag{2}$$

assuming that the air density is constant in the whole domain. We formulate a least-square problem in the domain Ω where the wind field $\vec{u}(\tilde{u}, \tilde{v}, \tilde{w})$ will be adjusted by the observed wind $\vec{v}_0(u_0, v_0, w_0)$, expressed as

$$E(\widetilde{u}, \widetilde{v}, \widetilde{w}) = \int_\Omega [\alpha_1^2 \Big((\widetilde{u} - u_0)^2 + (\widetilde{v} - v_0)^2 \Big) + \alpha_2^2 (\widetilde{w} - w_0)^2] \;\; d\Omega \qquad (3)$$

with α_1 and α_2 being the Gauss precision moduli. The solution $\vec{v}\,(u, v, w)$ is equivalent to find a saddle point $(\vec{v}, \phi)$ of Lagrangian [1]

$$\Upsilon(\vec{v}) = \min_{\vec{u} \in K} E(\vec{u}) + \int_\Omega \phi \vec{\nabla} \cdot \vec{u}\, d\Omega \qquad (4)$$

Lagrange multiplier technique is used to minimize problem (4), whose minimum comes to form the Euler-Lagrange equations,

$$u = u_0 + T_h \frac{\partial \phi}{\partial x} \qquad (5)$$

$$v = v_0 + T_h \frac{\partial \phi}{\partial y} \qquad (6)$$

$$w = w_0 + T_v \frac{\partial \phi}{\partial z} \qquad (7)$$

where ϕ is the Lagrange multiplier and $T = (T_h, T_h, T_v)$ is the diagonal transmissivity tensor,

$$T_h = \frac{1}{2\alpha_1^2} \quad \text{and} \quad T_v = \frac{1}{2\alpha_2^2} \qquad (8)$$

As α_1 and α_2 are constant in Ω, the variational approach results in an elliptic equation by substituting (5), (6) and (7) in (1),

$$\frac{\partial^2 \phi}{\partial x^2} + \frac{\partial^2 \phi}{\partial y^2} + \frac{T_v}{T_h} \frac{\partial^2 \phi}{\partial z^2} = -\frac{1}{T_h} \left(\frac{\partial u_0}{\partial x} + \frac{\partial v_0}{\partial y} + \frac{\partial w_0}{\partial z} \right) \qquad (9)$$

so the boundary conditions result as follows (Dirichlet condition on flow-through boundaries and Neumann condition on terrain and top),

$$\phi = 0 \qquad \text{on} \qquad \Gamma_a \qquad (10)$$

$$\vec{n} \cdot T \vec{\nabla} \phi = -\vec{n} \cdot \vec{v}_0 \qquad \text{on} \qquad \Gamma_b \qquad (11)$$

1.1 Terrain conformal coordinates

We propose the following conformal coordinate transformation which reduces the tridimensional domain to a unitary cube Ω', where the terrain is now represented as a horizontal plane,

$$\xi = \frac{x}{x_l}, \quad \eta = \frac{y}{y_l} \quad \text{and} \quad \sigma = \frac{z - z_s}{z_t - z_s} = \frac{z - z_s}{\pi} \tag{12}$$

Here, $z_s\,(x, y)$ is the function which define the terrain topography, z_t is the maximum height and both x_l and y_l are the maximum horizontal length of the domain. Let denote $\pi = z_t - z_s$. Then equation (8) becomes to

$$\frac{\pi}{x_l^2}\frac{\partial^2 \phi}{\partial \xi^2} + \frac{\pi}{y_l^2}\frac{\partial^2 \phi}{\partial \eta^2} + \left[\frac{(\sigma-1)^2}{\pi}\left(\left(\frac{\partial z_s}{\partial x}\right)^2 + \left(\frac{\partial z_s}{\partial y}\right)^2\right) + \frac{T_v}{T_h}\frac{1}{\pi}\right]\frac{\partial^2 \phi}{\partial \sigma^2}$$

$$+2(\sigma-1)\left[\frac{1}{x_l}\frac{\partial z_s}{\partial x}\frac{\partial^2 \phi}{\partial \xi \partial \sigma} + \frac{1}{y_l}\frac{\partial z_s}{\partial y}\frac{\partial^2 \phi}{\partial \eta \partial \sigma}\right]$$

$$+(\sigma-1)\left[\frac{\partial^2 z_s}{\partial x^2} + \frac{\partial^2 z_s}{\partial y^2} + \frac{2}{\pi}\left(\left(\frac{\partial z_s}{\partial x}\right)^2 + \left(\frac{\partial z_s}{\partial y}\right)^2\right)\right]\frac{\partial \phi}{\partial \sigma}$$

$$= -\frac{1}{T_h}\left[\pi\left(\frac{1}{x_l}\frac{\partial u_0}{\partial \xi} + \frac{1}{y_l}\frac{\partial v_0}{\partial \eta}\right) + (\sigma-1)\left(\frac{\partial u_0}{\partial \sigma}\frac{\partial z_s}{\partial x} + \frac{\partial v_0}{\partial \sigma}\frac{\partial z_s}{\partial y}\right) + \frac{\partial w_0}{\partial \sigma}\right]$$

Using the conformal transformation, the boundary conditions (10) and (11) yield

$$\phi = 0 \;\; \text{on} \;\; \Gamma_a \tag{13}$$

$$\frac{\partial \phi}{\partial \sigma} = 0 \;\; \text{on} \;\; \Gamma_{b_1} \tag{14}$$

$$\frac{\partial \phi}{\partial \sigma} = \frac{\frac{\pi}{T_h}\left[\left(u_0 + T_h\frac{1}{x_l}\frac{\partial \phi}{\partial \xi}\right)\frac{\partial z_s}{\partial x} + \left(v_0 + T_h\frac{1}{y_l}\frac{\partial \phi}{\partial \eta}\right)\frac{\partial z_s}{\partial y} - w_0\right]}{\left(\frac{\partial z_s}{\partial x}\right)^2 + \left(\frac{\partial z_s}{\partial y}\right)^2 + \frac{T_v}{T_h}} \;\; \text{on} \;\; \Gamma_{b_0} \tag{15}$$

where Γ_a being to the vertical faces of the boundary, $\Gamma_{b_1}(\sigma = 1)$ the top and $\Gamma_{b_0}(\sigma = 0)$ the bottom.

1.2 Initial wind profile

The technique for horizontal interpolation is formulated as a function of the inverse of the squared distance and the height difference between the point and the station [2],

$$\vec{v}_0(z_e) = \varepsilon\,\frac{\sum\limits_{n=1}^{N}\frac{\vec{v}_n}{d_n^2}}{\sum\limits_{n=1}^{N}\frac{1}{d_n^2}} + (1-\varepsilon)\,\frac{\sum\limits_{n=1}^{N}\frac{\vec{v}_n}{|\Delta h_n|}}{\sum\limits_{n=1}^{N}\frac{1}{|\Delta h_n|}} \tag{16}$$

where ε is a weighting parameter $(0 \leq \varepsilon \leq 1)$, which allows to give more importance to one of these two criteria. The value of $\vec{v}_n$ is the velocity observed at the station n, where N is the number of stations considered in the interpolation, d_n is the horizontal distance from station n to the point of the domain where we are computing the wind velocity, $|\Delta h_n|$ is the height difference between station n and the studied point.

In this work, a log-linear wind profile is considered [3] at the surface layer, which takes into account the horizontal interpolation and the effect of roughness on the wind intensity and direction. These values also depend on the air stability (neutral, stable or unstable atmosphere) according to the Pasquill stability class. Above the surface layer, a linear interpolation is carried out using the geostrophic wind. The logarithmic profile is given by,

$$\vec{v}_0(z) = \frac{\vec{v}^*}{k}\left(\log\frac{z}{z_0} - \Phi_m\right) \qquad z_0 < z \leq z_{sl} \tag{17}$$

where $\vec{v}^*$ is the friction velocity, k is the von Karman's constant, z_0 is the roughness length [4], z_{sl} is the height of the surface layer and Φ_m depends on the air stability,

$$\begin{aligned}
&\Phi_m = 0 && \text{(neutral)} \\
&\Phi_m = -5\frac{z}{L} && \text{(stable)} \\
&\Phi_m = \log\left[\left(\frac{\theta^2+1}{2}\right)\left(\frac{\theta+1}{2}\right)^2\right] - 2\arctan\theta + \frac{\pi}{2} && \text{(unstable)}
\end{aligned} \tag{18}$$

being,

$$\theta = (1-16\frac{z}{L})^{1/4} \qquad \text{and} \qquad \frac{1}{L} = a z_0^b \tag{19}$$

with a and b depending on the Pasquill stability class (see e.g.[5]). The friction velocity is obtained at each point from the interpolated measurements at the height of the stations (horizontal interpolation),

$$\vec{v}^* = \frac{k\ \vec{v}_0(z_e)}{\ln\frac{z_e}{z_0} - \Phi_m} \tag{20}$$

The height of boundary layer z_{pbl} above the ground is computed such that the wind intensity and direction are constant at that height (geostrophic wind) is,

$$z_{pbl} = \frac{\gamma\,|\vec{v}^*|}{f} \tag{21}$$

where $f = 2\Theta\ \sin\phi$ is the Coriolis parameter (Θ is the earth rotation velocity and ϕ the latitude), and γ is a parameter depending on the atmospheric stability between 0.15 and 0.3.

The height of the mixed layer h is considered to be equal to z_{pbl} in neutral and unstable conditions. In stable conditions, it is approximated by

$$h = \gamma' \sqrt{\frac{|\vec{v}^*|\, L}{f}} \tag{22}$$

where $\gamma' = 0.4$ [6,7]. The height of surface layer is $z_{sl} = \frac{h}{10}$. From z_{sl} to z_{pbl}, a linear interpolation with geostrophic wind $\vec{v}_g$ is carried out,

$$\vec{v}_0(z) = \rho(z)\, \vec{v}_0(z_{sl}) + [1 - \rho(z)]\vec{v}_g \qquad \text{if} \qquad z_{sl} < z \leq z_{pbl} \tag{23}$$

where $\rho(z)$ is

$$\rho(z) = 1 - \left(\frac{z - z_{sl}}{z_{pbl} - z_{sl}}\right)^2 \left(3 - 2\frac{z - z_{sl}}{z_{pbl} - z_{sl}}\right) \tag{24}$$

Finally, the model considers

$$\vec{v}_0(z) = \vec{v}_g \qquad \text{if} \qquad z > z_{pbl} \tag{25}$$

$$\vec{v}_0(z) = 0 \qquad \text{if} \qquad z \leq z_0 \tag{26}$$

2 Air pollution modelling

In an Eulerian model, the convection-diffusion-reaction equation for a pollutant species i is formulated as (see e.g.[8]),

$$\frac{\partial c_i}{\partial t} + \vec{v} \cdot \vec{\nabla} c_i - \vec{\nabla} \cdot (\mathbf{K}_i \vec{\nabla} c_i) = f_i \qquad i = 1, ..., p, \qquad \text{in} \quad \Omega \tag{27}$$

where p is the number of pollutant species, $c_i = c_i(x_1, x_2,\ x_3, t)$ represents the average concentration of pollutant i, $\vec{v}$ is the wind velocity computed with the previous model, $K_i = [K_{i1}(x_1, x_2, x_3)\ ,\ K_{i2}(x_1, x_2, x_3),\ K_{i3}(x_1, x_2, x_3)]$ is the diagonal tensor of diffusivity and $f_i = f_i(c_1, c_2, ..., c_p)$ is the source term. We suppose that the initial value of c_i, for $i = 1, ..., p$, is known in Ω,

$$c_i(x_1, x_2, x_3, 0) = c_i^0(x_1, x_2, x_3) \qquad i = 1, ..., p, \qquad \text{in} \quad \Omega \tag{28}$$

as well as the boundary conditions in Γ_a and Γ_b,

$$c_i = C_i(x_1, x_2, x_3, t) \qquad i = 1, ..., p, \qquad \text{in} \quad \Gamma_a \tag{29}$$

$$-\vec{n} \cdot \mathbf{K}_i \vec{\nabla} c_i = 0 \qquad i = 1, ..., p, \qquad \text{in} \quad \Gamma_{b1} \tag{30}$$

$$-\vec{n} \cdot \mathbf{K}_i \vec{\nabla} c_i = v_{di} c_i \qquad i = 1, ..., p, \qquad \text{in} \quad \Gamma_{b0} \tag{31}$$

where v_{di} is the dry deposition velocity over the terrain. In general, C_i will be considered equal to zero or to the environmental value.

2.1 *The source of pollutants*

If the chemistry of the species and the wet deposition are taken into account in the model, the source term of equation (27) becomes to [9],

$$f_i = E_i + R_i + P_i = E_i + \sum_{j=1}^{p} \alpha_{ij}\ c_j \tag{32}$$

where $E_i(x_1, x_2, x_3, t)$ is the direct emission of species i, $R_i(x_1, x_2, x_3, t)$ represents the variation of the concentration of species i due to chemical reactions and $P_i(x_1, x_2, x_3, t)$ is the elimination by precipitations (wet deposition). The model assumes that R_i and P_i are lineal. The emission of a chimney located at (x_{01}, x_{02}, x_{03}) has been approached by,

$$E_i = \frac{C_{i_0}(2\pi)^{-3/2}}{\sigma_x \sigma_y \sigma_z} \exp\left\{-\left[\left(\frac{x_1 - x_{1_0}}{\sqrt{2}\sigma_x}\right)^2 + \left(\frac{x_2 - x_{2_0}}{\sqrt{2}\sigma_y}\right)^2 + \left(\frac{x_3 - x_{3_0}}{\sqrt{2}\sigma_z}\right)^2\right]\right\} \tag{33}$$

We have considered NO_x, HNO_3, SO_2 and H_2SO_4 the significant species, simplifying the nonlinear module of reactions [10] leads to these linear terms (see e.g. [11]),

$$R_{NO_x} = \overline{\alpha}_{NO_x,NO_x}\ c_{NO_x} \tag{34}$$
$$R_{HNO_3} = -\overline{\alpha}_{NO_x,NO_x}\ c_{NO_x} \tag{35}$$
$$R_{SO_2} = \overline{\alpha}_{SO_2,SO_2}\ c_{SO_2} \tag{36}$$
$$R_{H_2SO_4} = -\overline{\alpha}_{SO_2,SO_2}\ c_{SO_2} \tag{37}$$

with

$$\overline{\alpha}_{NO_x,NO_x} = -2\, k_1\, k_2 \tag{38}$$
$$\overline{\alpha}_{SO_2,SO_2} = -2\, \frac{k_1\, k_3}{k_2} \tag{39}$$

where k_1, k_2 and k_3 are kinetic parameters corresponding to,

$$NO_2 + h \cdot v \xrightarrow{1} NO + O\cdot$$

$$OH \cdot + NO_2 \xrightarrow{2} HNO_3$$
$$OH \cdot + SO_2 \xrightarrow{3} HOSO_2\cdot$$

The contribution of the wet deposition is formulated by a linear term too,

$$P_i = -\frac{v_{wi}}{h}\, c_i = -\frac{w_{ri}}{h}\, p_0 c_i \tag{40}$$

being h the average mixed layer and v_{wi} the velocity of wet deposition defined as

$$v_{wi} = w_{ri}\, p_0 \tag{41}$$

where w_{ri} is the proportion on the surface between the concentration of precipitated materia and the concentration of materia in the air, and p_0 is the intensity of precipitation. Thus, the coefficients of equation (32) become to,

$$\begin{aligned} \alpha_{ij} &= \overline{\alpha}_{ij} \;\text{ if }\; j \neq i \\ \alpha_{ii} &= \overline{\alpha}_{ii} - \frac{v_{wi}}{h} \end{aligned} \tag{42}$$

2.2 High-order accurate time-stepping scheme

Following the technique developed by Lax and Wendroff [12], a general formulation for the convection-diffusion-reaction equation is proposed. It is based on a high order time discretization by means of the Taylor's span combined with a finite difference discretization [13]. Nowadays a similar technique, but using Galerkin finite elements leads to the so called Taylor-Galerkin schemes [14–16]. Thus, we have for the species i,

$$c_i^{n+1} = c_i^n + \Delta t \left.\frac{\partial c_i}{\partial t}\right|_n + \frac{\Delta t^2}{2} \left.\frac{\partial^2 c_i}{\partial t^2}\right|_{n+\theta} + O(\Delta t^3) \tag{43}$$

From equation (27), the first time derivative $\frac{\partial c_i}{\partial t}$ may be expressed in terms of spatial derivatives, and $\frac{\partial^2 c_i}{\partial t^2}$ may be approached from the time derivation of equation (27) (see e.g. [17]). The new formulation of equation (43) results in,

$$\begin{aligned} &\left[1 - \frac{\Delta t^2}{6}\left((\vec{v}\cdot\vec{\nabla})\vec{v}\cdot\vec{\nabla} + \vec{v}\cdot(\vec{v}\cdot\vec{\nabla})\vec{\nabla}\right) - \Delta t \mathbf{K}_i \nabla^2\right]\left(\frac{c_i^{n+1}-c_i^n}{\Delta t}\right) \\ &-\left[\frac{\Delta t}{2}\alpha_{i1} - \frac{5}{12}\Delta t^2 \alpha_{i1}\vec{v}\cdot\vec{\nabla}\right]\left(\frac{c_1^{n+1}-c_1^n}{\Delta t}\right) \\ &-\left[\frac{\Delta t}{2}\alpha_{i2} - \frac{5}{12}\Delta t^2 \alpha_{i2}\vec{v}\cdot\vec{\nabla}\right]\left(\frac{c_2^{n+1}-c_2^n}{\Delta t}\right) \end{aligned}$$

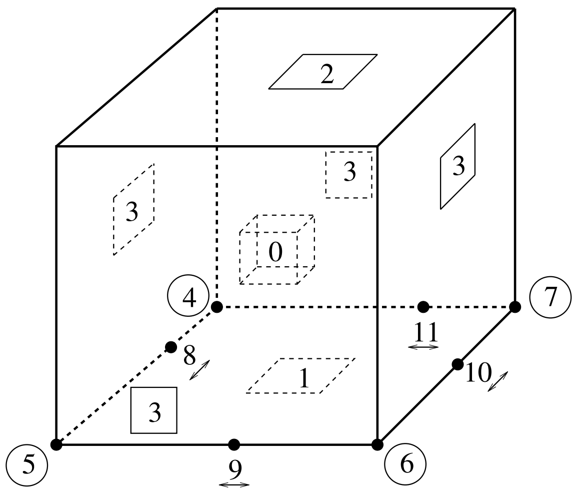

Fig. 1. Reference numbers in the unitary cube

$$
\begin{aligned}
&= -\vec{v}\cdot\vec{\nabla}c_i^n + \frac{\Delta t}{2}(\vec{v}\cdot\vec{\nabla})\vec{v}\cdot\vec{\nabla}c_i^n + \frac{\Delta t}{2}\vec{v}\cdot(\vec{v}\cdot\vec{\nabla})\vec{\nabla}c_i^n \\
&-\frac{\Delta t}{2}\left(\mathbf{K}_i\nabla^2\vec{v}\right)\cdot\vec{\nabla}c_i^n + \frac{\Delta t^2}{6}\vec{v}\cdot\vec{\nabla}\left(\vec{v}_t\cdot\vec{\nabla}c_i^n\right) + \mathbf{K}_i\nabla^2 c_i^n \\
&-\frac{\Delta t}{2}\vec{v}\cdot\vec{\nabla}E_i - \frac{\Delta t}{2}\alpha_{i1}\mathbf{K}_i\nabla^2 c_1^n - \frac{\Delta t}{2}\alpha_{i1}E_1 - \frac{\Delta t}{2}\alpha_{i1}\alpha_{11}c_1^n \\
&-\frac{\Delta t}{2}\alpha_{i1}\alpha_{12}c_2^n - \frac{\Delta t}{2}\alpha_{i2}\mathbf{K}_i\nabla^2 c_2^n - \frac{\Delta t}{2}\alpha_{i2}E_2 - \frac{\Delta t}{2}\alpha_{i2}\alpha_{21}c_1^n \\
&-\frac{\Delta t}{2}\alpha_{i2}\alpha_{22}c_2^n - \frac{\Delta t^2}{6}\vec{v}\cdot\vec{\nabla}E_{it} + E_i + \alpha_{i1}c_1^n + \alpha_{i2}c_2^n - \frac{\Delta t}{2}\mathbf{K}_i\nabla^2 f_i \\
&+O(\Delta t^3, \|\mathbf{K}_i\|\,\Delta t^2, \|\mathbf{K}_i\|^2\,\Delta t)
\end{aligned}
\qquad (44)
$$

3 Finite difference discretization

Before applying finite differences for the spatial discretization, equation (44) is transformed using the conformal coordinate system (12). The selected finite difference scheme depends on the node location. We have related each location to a reference number, as shown in Figure 1. From here, a mesh with regular horizontal spacing is considered. However, in the vertical direction, the spacing could be variable.

For the inner points, whose reference number is 0, the schemes proposed for the $c(x_{1i}, x_{2j}, x_{3k}, t)$ derivatives are,

$$\frac{\partial\phi}{\partial\xi} = \frac{\phi_{i+1,j,k} - \phi_{i-1,j,k}}{2\Delta\xi} + O(\Delta\xi^2) \qquad (45)$$

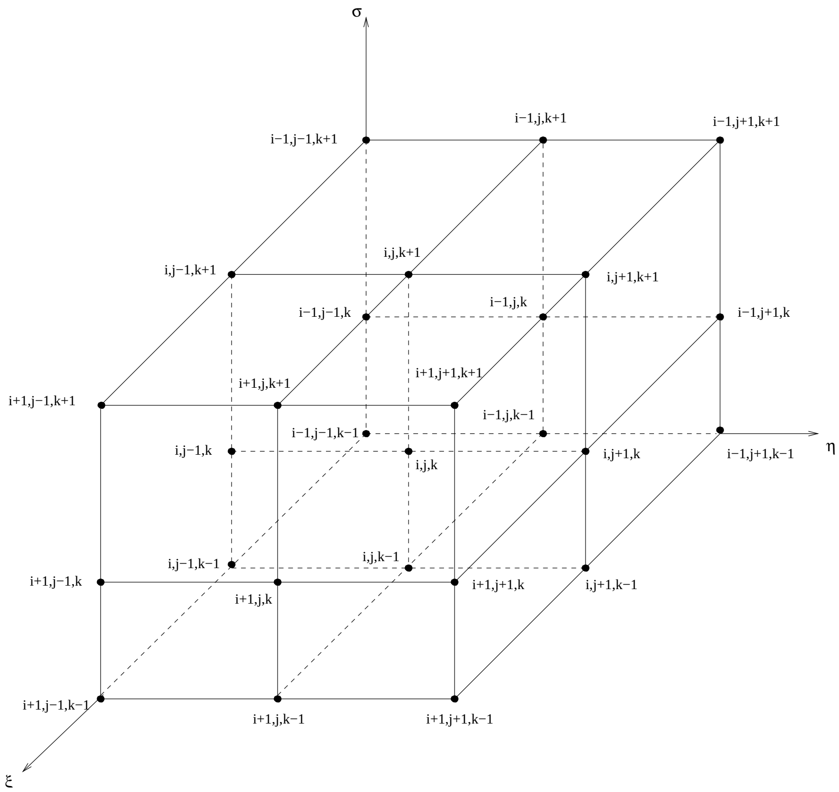

Fig. 2. Inner nodes molecule. There are 15 nodes for wind modelization, while in the pollutant model for the first pollutant species ($i = 1$) there are 19 nodes, and 26 nodes for the second one ($i = 2$).

$$\frac{\partial \phi}{\partial \eta} = \frac{\phi_{i,j+1,k} - \phi_{i,j-1,k}}{2\Delta\eta} + O(\Delta\eta^2) \tag{46}$$

$$\frac{\partial \phi}{\partial \sigma} = \frac{\lambda_k^2 \phi_{i,j,k+1} - (\lambda_k^2 - 1)\phi_{i,j,k} - \phi_{i,j,k-1}}{\Delta\sigma_k^+ (\lambda_k + \lambda_k^2)} + O(\lambda_k \Delta{\sigma_k^+}^2) \tag{47}$$

$$\frac{\partial^2 \phi}{\partial \xi^2} = \frac{\phi_{i-1,j,k} - 2\phi_{i,j,k} + \phi_{i+1,j,k}}{\Delta\xi^2} + O(\Delta\xi^2) \tag{48}$$

$$\frac{\partial^2 \phi}{\partial \eta^2} = \frac{\phi_{i,j-1,k} - 2\phi_{i,j,k} + \phi_{i,j+1,k}}{\Delta\eta^2} + O(\Delta\eta^2) \tag{49}$$

$$\frac{\partial^2 \phi}{\partial \sigma^2} = 2\frac{\phi_{i,j,k-1} - (1+\lambda_k)\phi_{i,j,k} + \lambda_k \phi_{i,j,k+1}}{\Delta{\sigma_k^+}^2 (\lambda_k + \lambda_k^2)} - \frac{1}{3}(\Delta\sigma_k^+ - \Delta\sigma_k^-) \frac{\partial^3 \phi}{\partial \sigma^3} + O(\Delta{\sigma_k^+}^2 - \Delta\sigma_k^- \Delta\sigma_k^+ + \Delta{\sigma_k^-}^2) \tag{50}$$

$$\frac{\partial^2 \phi}{\partial \xi \partial \eta} = \frac{\phi_{i+1,j+1,k} - \phi_{i-1,j+1,k} - \phi_{i+1,j-1,k} + \phi_{i-1,j-1,k}}{4\Delta\xi\Delta\eta} + O(\Delta\xi^2, \Delta\eta^2) \tag{51}$$

$$\frac{\partial^2 \phi}{\partial \xi \partial \sigma} = \frac{\lambda_k^2 \phi_{i+1,j,k+1} - \lambda_k^2 \phi_{i-1,j,k+1} - \phi_{i+1,j,k-1} + \phi_{i-1,j,k-1}}{2\Delta\sigma_k^+ (\lambda_k + \lambda_k^2)\Delta\xi} + \frac{(\lambda_k^2 - 1)\phi_{i-1,j,k} - (\lambda_k^2 - 1)\phi_{i+1,j,k}}{2\Delta\sigma_k^+ (\lambda_k + \lambda_k^2)\Delta\xi} + O(\Delta\xi^2, \lambda_k \Delta{\sigma_k^+}^2) \tag{52}$$

$$\frac{\partial^2 \phi}{\partial \eta \partial \sigma} = \frac{\lambda_k^2 \phi_{i,j+1,k+1} - \lambda_k^2 \phi_{i,j-1,k+1} - \phi_{i,j+1,k-1} + \phi_{i,j-1,k-1}}{2\Delta\sigma_k^+ (\lambda_k + \lambda_k^2)\Delta\eta} + \frac{(\lambda_k^2 - 1)\phi_{i,j-1,k} - (\lambda_k^2 - 1)\phi_{i,j+1,k}}{2\Delta\sigma_k^+ (\lambda_k + \lambda_k^2)\Delta\eta} + O(\Delta\eta^2, \lambda_k \Delta{\sigma_k^+}^2) \tag{53}$$

being $\lambda_k = \frac{\Delta\sigma_k^-}{\Delta\sigma_k^+}$.

All the schemes are second order, except the corresponding one to $\frac{\partial^2 c}{\partial \sigma^2}$, which is second order in the case of regular vertical spacing $\left(\Delta\sigma_k^+ = \Delta\sigma_k^-\right)$, or if it is defined in a proper manner to be second order. In our case we have used $\Delta\sigma_k^+ = \Delta\sigma_k^- + \Delta{\sigma_k^-}^2$ which produces more concentration of points near the terrain.

On the boundary, second order schemes are also proposed for the first derivatives of c and for the derivatives of z_s, using the same technique as [18]. Thus the elliptic equation (13) and the boundary conditions (13), (14) and (15) are discretized by the schemes referenced before.

As the resulting system of equations $Ax = b$ is non-symmetric, a suitable linear solver should be applied. In our case, the Bi-CGSTAB biorthogonalization algorithm [19] has been used, since this method has proved its efficiency to solve this type of linear systems of equations, which arises from the finite difference discretization. To improve the convergence, several classical preconditioners, like $diag(A)$, $SSOR(w)$ and $ILU(0)$ [20] have been implemented.

4 Numerical experiment

The studied region has been located at the south of La Palma Island (Canary Islands). A $31200m \times 31200m \times 4000m$ domain Ω has been selected, being $2150m$ the maximum height above sea level. The necessary data for wind field adjustment has been obtained from [21], and summarized in Table 1, with $\vec{v_g} = (-38.5, 3.40, 0.00)\ m/s$ and $D\ (neutral)$ Pasquill stability class.

Once the wind field is known (see Figure 3) and for our $81 \times 81 \times 21$ mesh we calculate the pollutant concentration in every node, from a $2n$ order system of equations (i.e. 275562 equations), preconditioned with $ILU(0)$. The tolerance was $\epsilon = 10^{-13}$.

The emission of pollutant, that follows a Gaussian model (see equation 33), is uniform throughout the time. The concentrations of pollutant grow up in the chimney from a null value, as it can see at Figure 4. For this experiment we have used $C_{i_0} = 10^6 g/s$, $\sigma_x = \sigma_y = 500$ y $\sigma_z = 50$, and $(x_{1_0}, x_{2_0}, x_{3_0}) =$

February 11, 1995		MBI	$MBII$	$MBIII$	LPA
$Coord$	X	227270.00	227155.00	227564.00	231715.00
	Y	3161499.00	3161564.00	3161443.00	3168209.00
	Z	460.00	475.00	390.00	40.00
$7:30\ a.m.$	Mod	5.68	5.8	6.85	8.89
	Dir	11.00	95.6	1.40	32.00

Table 1
Meteorological station locations in UTM (*Universal Transversal Mercator*). Wind modules are in m/s and the wind directions in north degrees.

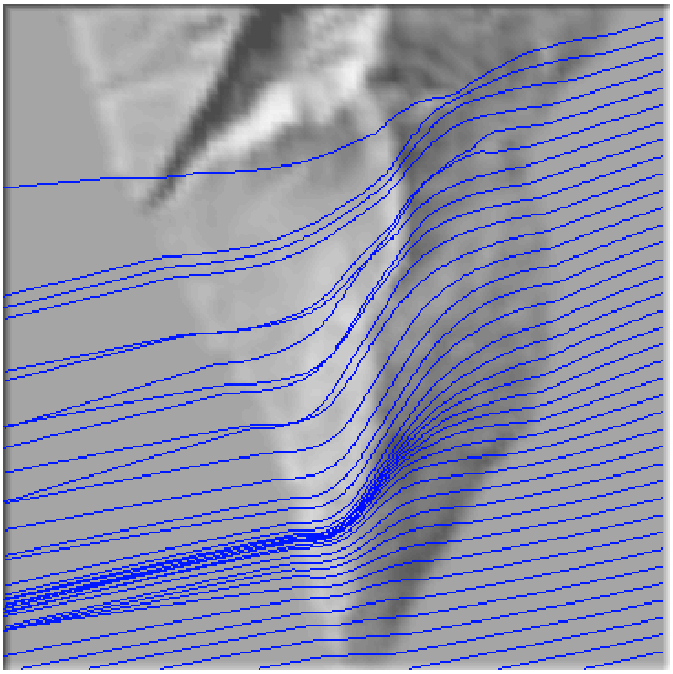

Fig. 3. Wind field isolines into the Ω domain, using Table 1 data.

$(230460, 3175133, 293.18)$ that are the coordinates of chimney (the heigh is over sea level).

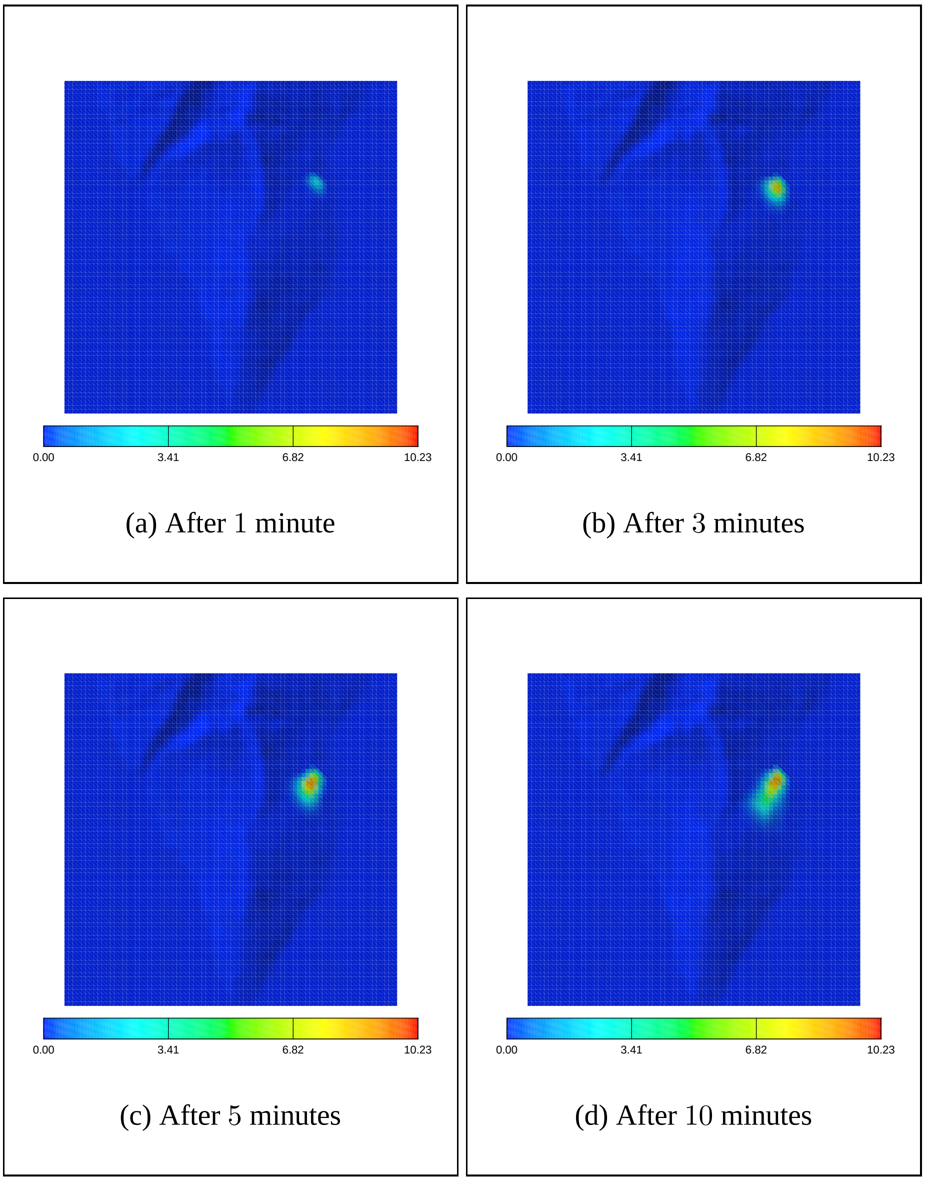

(a) After 1 minute (b) After 3 minutes (c) After 5 minutes (d) After 10 minutes

Fig. 4. H_2SO_4 propagation at the chimney height.

5 Conclusion

In this work a consistent mass model has been developed to adjust 3-D wind fields. From these we construct an air pollution model to approach the concentration of two set of coupled species: NO_x, HNO_3, and SO_2, H_2SO_4. The use of a terrain conformal coordinate system allows to construct a simpler mesh due to the elimination of irregularities of the terrain. Though, in general, the variable vertical spacing leads to schemes of first consistence order, some strategies, here proposed, lead to second order schemes. Thus, the proposed formulation for the convection-diffusion-reaction problem provides interesting properties of consistence and stability. The model does not only allow to generate wind maps from the measurements obtained in few stations, but to obtain the history of a pollution episode for the considered species.

References

[1] Winter, G., Montero, G., Ferragut, L., Montenegro, R. (1995). Adaptive strategies using standard and mixed finite elements for wind field adjustment. *Solar Energy*, v. 54, 1, pp. 49-56.

[2] Montero, G., Montenegro, R., Escobar, J.M. (1998). A 3-D Model for Wind Field Adjustment.*J. Wind. Eng. and Ind. Aerd.*, v. 76-46, pp. 249-261.

[3] Lalas, D.P., Ratto, C.F. (1996). Modelling of Atmospheric Flow Fields. World Scientific Publishing, Singapore.

[4] McRae, G.J., Goodin, W.R., Seinfeld, J.H. (1982). Development of a second generation mathematical model for urban air pollution I. Model formulation. *Atm. Env.*, v. 16, 4, pp. 679-696.

[5] Zannetti, P. (1990). *Air Pollution Modeling*. Comput. Mech. Publ., Boston.

[6] Garratt, J.R. (1982). Observations in the nocturnal boundary layer,*Boundary Layer Meteorol.*, v.22, pp. 24-48.

[7] Panofsky, H.A., Dutton, J.A. (1984). Atmosfheric Turbulence, Models and Methods for Enginnering Applications. John Wiley, New York.

[8] Graziani, G. (1994). Survey of long range transport models, en *Environmental Modeling Vol. II, Computer Methods and Software for Simulating Environmental Pollution and its Adverse Effects*, P. Zannettti, Ed., pp. 103-142.

[9] Winter, G., Betancor, J., Montero, G. 3D Simulation in the lower troposphere: Wind field adjustment to observational data and dispersion of air pollutants from combustion of sulfur-containing fuel, in J.I.Daz(ed), Ocean circulation and pollution control - A mathematical and numerical investigation, Springer Berlin-Heidelberg, pp. 29-51, 2004.

[10] Seinfeld, J.H. (1986). *Atmospheric Chemistry and Physics of Air Pollution*, John Wiley & Sons, New York.

[11] Mata, L.J., García, R., Santana, R. (1994). Simulating acid deposition in tropical regions, en Air Pollution II Volume 2: Pollution Control and Monitoring, J.M. Baldasano, C.A. Brebbia, H. Power y P. Zannetti, Eds., Comput. Mech. Publ., Boston, pp. 59-67.

[12] Lax, P.D., Wendroff, B. (1960). Systems of conservative laws, *Comm. Pure Appl. Math.*, 13, pp. 217-237.

[13] Sanín, N., Montero, G. (2001). Un esquema de alto orden en tiempo para la modelizacin 3-D del transporte de contaminantes en la atmsfera, Proc. Cedya 2001, eds. Ferragut, L., Santos, A. Salamanca.

[14] Donea, J., Roig, B., and Huerta, A. (2000). High Order Accurate Time-Stepping Schemes for Convection-Diffusion Problems, *Comput. Meths. Appl. Mech. Engg*, v. 182, pp. 249-275.

[15] Donea, J., Roig, B., and Huerta, A. (2002). Time-accurate solution of stabilized convection-diffusion-reaction equations: I time and space discretization, *Comput. Meths. Appl. Mech. Engg*, v. 18, pp. 565-573.

[16] Donea, J., Roig, B., and Huerta, A. (2002). Time-accurate solution of stabilized convection-diffusion-reaction equations: II accuracy analysis and examples, *Comput. Meths. Appl. Mech. Engg*, v. 18, pp. 575-584.
[17] Donea, J. (1984). A Taylor-Galerkin method for convective transport problems, *Int. J. Num. Meth. Eng.*, 20, pp. 101-119.
[18] Sanín, N., Montero, G. (1999). Construccin de un modelo tridimensional para ajuste de campos de viento mediante diferencias finitas. *Proc. of the CEDYA'99*, eds. R. Montenegro, G. Montero & G. Winter, Publications of Las Palmas de Gran Canaria University: Las Palmas de Gran Canaria, pp.1603-1612.
[19] van der Vorst, H.A. (1992). BI-CGSTAB: a fast and smoothly converging variant of BI-CG for the solution of nonsymmetric linear systems, *SIAM J. Sci. Statist. Comput.*, v. 13, pp. 631-644.
[20] Martin, G. (1991). Methodes de preconditionnemen par factorisation incomplete, *Memoire de Maitrise*, Universite Laval, Quebec, Canada.
[21] Montero, G., Sanín, N. (2001). Modelling of Wind Field Adjustment Using Finite differences in a Terrain Conformal Coordinate System. *J. Wind. Eng. and Ind. Aerd.*, v. 89, pp. 471-488.